Design of Wingtip Devices for Marine Applications

Timothy Barrett
Aleksandra Wojtowicz

Advisors:
Ivaylo Nedyalkov
Martin Wosnik

Abstract

Wingtip devices can decrease wing tip vortex strength, and thereby improve the performance of marine turbines and vehicles. The goal of the project is to design wingtip devices for marine applications and evaluate their lift, drag, and cavitation characteristics. The performance of different baseline wingtip devices was characterized using the open source computational fluid dynamics (CFD) software OpenFOAM. The results were validated through experimental testing in the UNH high speed cavitation tunnel (HiCaT). New wingtip devices were developed and studied numerically. A physical model of a potential device will be built and tested experimentally.

Table of Contents

List of Figures 3

List of Tables 5

1. Introduction 6

2. Theory 7

    2.1. Hydrofoil Designs 7

    2.2. New Design – Twist Tip 7

3. Numerical Analysis 9

4. Experimental Analysis 11

    4.1. High-Speed Cavitation Tunnel (HiCaT) 11

    4.2. Tunnel Calibration 12

    4.3. Dynamic Response 14

    4.4. Drag Plate Studies 21

5. Results 22

6. Conclusions 24

7. Future Development 25

8. References 26

9. Acknowledgments 27

10. Appendix 28

    10.1. OpenFOAM Figures 28

    10.2. MATLAB Code 32

List of Figures

Figure 1: Images of End Cap Foil (left), General Foil (middle), Split Tip (right)..... 7

Figure 2: Parameters of wingtip geometry..... 7

Figure 3: Twist Tip 8

Figure 4: Computational analysis of the Twist Tip..... 10

Figure 5: HiCaT located in Chase Ocean Engineering Laboratory..... 11

Figure 6: LabView user interface..... 12

Figure 7: Digital level set up..... 13

Figure 8: Mass-string pulley system used for calibration..... 13

Figure 9: Formation and shedding of cavitation..... 14

Figure 10: Force balance in the HiCaT tunnel..... 14

Figure 11: Drag force balance with the seal (right) and without (left)..... 14

Figure 12: Mechanical Second Order System schematics..... 15

Figure 13: Mass-string pulley system simulating a fully reversed load on the sensor..... 16

Figure 14: Drag sensor on the tunnel..... 16

Figure 15: Force balance curve with seal (right) and without seal (left)..... 17

Figure 16: Dynamic response of the system with & without seal with a known mass of 500 g.... 18

Figure 17: Frequency response Bode plot of the system..... 19

Figure 18: Lift dynamic response of the system..... 20

Figure 19: Force balance calibration with the old drag plate and the new drag plate..... 21

Figure 20: The numerical and experimental comparison of lift and drag coefficients of the end cap as a function of the angle of attack..... 22

Figure 21: The numerical and experimental comparison of lift and drag coefficients of the general foil as a function of the angle of attack.....23

Figure 22: The numerical and experimental comparison of lift and drag coefficients of the split tip as a function of the angle of attack..... 23

Figure 23: OpenFOAM image showing vorticity in the streamlines and the pressure distribution across the End Cap Foil..... 28

Figure 24: OpenFOAM image showing vorticity in the cross sections and the pressure distribution across the End Cap Foil..... 28

Figure 25: OpenFOAM image showing vorticity in the streamlines and the pressure distribution across the General Foil..... 29

Figure 26: OpenFOAM image showing vorticity in the cross sections and the pressure distribution across the General Foil..... 29

Figure 27: OpenFOAM image showing vorticity in the streamlines and the pressure distribution across the Split Tip..... 30

Figure 28: OpenFOAM image showing vorticity in the cross sections and the pressure distribution across the Split Tip..... 30

Figure 29: OpenFOAM image showing vorticity in the streamlines and the pressure distribution across the Twist Tip..... 31

Figure 30: OpenFOAM image showing vorticity in the cross sections and the pressure distribution across the Twist Tip..... 31

List of Tables

Table 1: System parameters..... 15

Table 2: Experimental natural frequency and damping ratio values..... 17

Table 3: Experimental Response time, settling time and frequency of oscillation..... 19

1 Introduction

Wingtip devices are widely used in the aerospace industry. As air flows around foils (e.g., wings or blades) lift is generated due to the higher pressure on one side of the foil and lower pressure on the other side. Near the tip of the airfoil however, air can start moving from one side of the wing to the other, generating wing tip vortices. As a result, the lift decreases near the tip of the wing, and in addition, drag is generated due to the significant amounts of energy dissipated by the wingtip vortices. Similar concept can be applied in marine environment with applications in marine turbines and marine vehicles. The major difference in the marine environment is the effect of cavitation. Cavitation is the formation of vapor in a liquid in regions of low pressure, and can be detrimental in marine applications (e.g., it can quickly damage turbines and propellers). It initially forms at the tip of the hydrofoil, however if the pressure continues to drop it will begin forming on the surface. As cavitation forms on the surface of the foil it continuously cycles through shedding and reforming. This causes oscillations which fatigues the system. Furthermore, cavitation id detrimental to the performance of marine devices and can be destructive to anything downstream due to the implosion of cavitation bubbles upon impact.

The main goal of this project was to design and test wingtip devices which improve performance by controlling cavitation and decreasing the size of wingtip vortices while avoiding bio-fouling and its effects. The project consisted of three major parts

- Theoretical
  Investigation of existing information about wingtip devices, tidal turbines, bio-fouling, cavitation, fluid dynamics in general, past project documentation.
- Numerical
  Comparison of various wingtip devices through numerical analysis using the state-of-the-art software for computational fluid dynamics (CFD) OpenFOAM.
- Experimental
  Testing of the wingtip devices in the High-Speed Cavitation Tunnel (HiCaT) at Chase Engineering building. As part of the experimental study, a new wingtip device has been modelled and numerically tested. The new design is currently being manufactured using Laser Metal Sintering.

2 Theory

2.1 Hydrofoil Designs

All hydrofoils were designed with the span measuring 3.25" which resulted in the wing centered in the test section. This in turn limited the effects of boundary conditions at the wall. The chord length was maximized in order to maximize the measurable lift forces.

End Cap Foil - The end cap foil was used as the baseline.

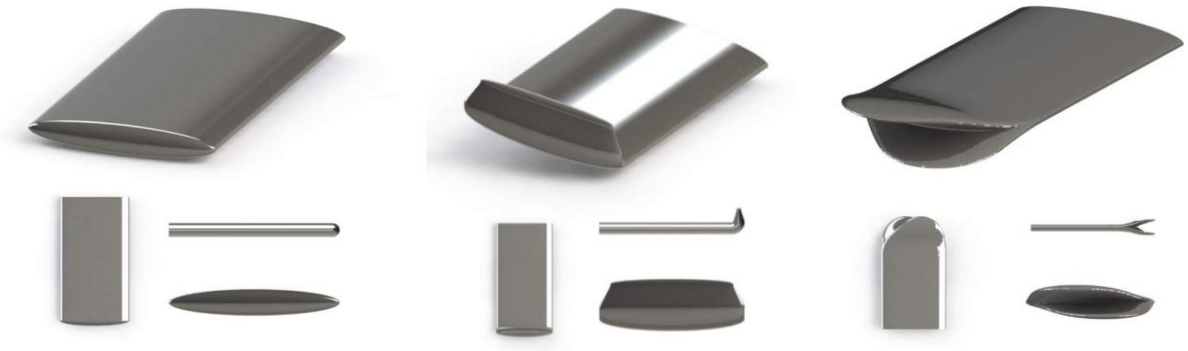

Figure 1: Images of End Cap Foil (left), General Foil (middle), Split Tip (right).

General Foil - The general foil limits the liquid flow from the high to the low pressure side. This delays the formation of cavitation, which in turns allows for a higher speed flows.

Split Tip - The split tip works by creating counter vortices. Theoretically, the vortices should cancel one another out, resulting in high reduction of cavitation.

2.2 New Design – Twist Tip

There are six key parameters that are used to describe the geometry of a wingtip: the winglet height, sweep angle, cant angle, curvature radius, toe angle, and twist angle. Those parameters are shown in Figure 2.

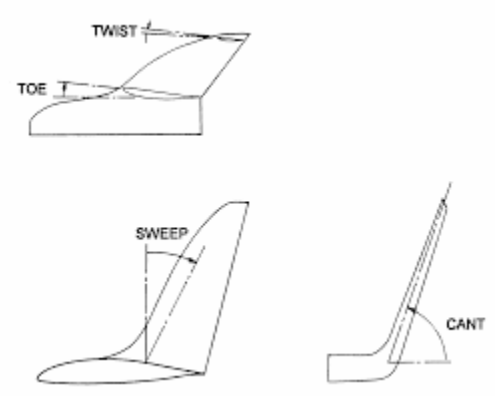

Figure 2: Parameters of wingtip geometry [2].

Jeppe Johansen and Niels N. Sorensen in their paper titled *'Aerodynamic investigation of Winglets on Wind Turbine Blades using CFD'* [2] investigated the importance and effects of several variations of the wingtip geometry by alternating various angles. They performed an in-depth analysis of the winglet height, curvature radius, and the sweep angle. They have determined that the mechanical power and thrust increases as curvature radius decreases, sweeping the wingtip 30° backwards does not increase mechanical power and that the mechanical power and thrust increases as winglet height increases. Based on the suggestions stated in the paper, new wingtip designs were evaluated. The design requirements for a new wingtip device for this project were to improve the performance of hydrofoils, increase the dynamic efficiency, decrease the size of wingtip vortices and the total drag, and to avoid bio-fouling. The new design, shown in Figure 3, was a modification of the general foil as the geometry of the general foil was easy to manufacture and not prone to bio-fouling. The wingtip was tapered in order to decrease the friction drag. The twist angle was adjusted from 0° - 6° in intervals of 2°. The performance of the twist tip was analyzed in OpenFoam and the results of the analysis are discussed in Section 3.

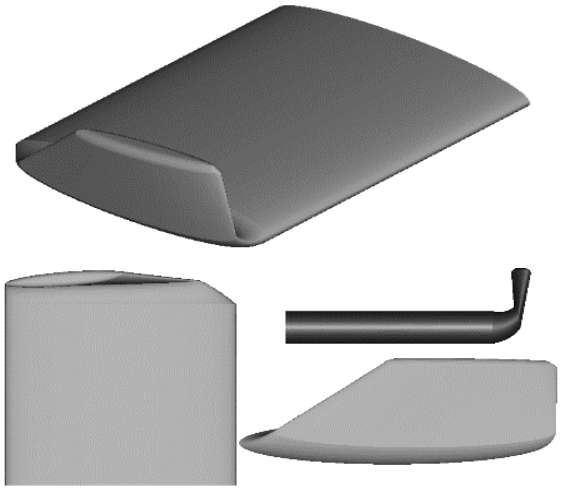

Figure 3: Twist Tip

3 Numerical Analysis

An integrated engineering approach towards design optimization was taken for this project. This process begins by reviewing theory and becoming familiar with existing wingtips before moving onto numerical and experimental testing. For this project open sourced computational fluid dynamics (CFD) software OpenFOAM was used to simulate the experimental testbed within the HiCaT tunnel. This software has high processing capabilities, is free, and can be used for many potential applications. The simulations created for this report represented a 6" x 6" x 36" flow section with a foil placed within it. OpenFOAM has the ability to produce C_{lift} and C_{drag} data for foils as well as show fluid flow data such as velocity, pressure, vorticity and more.

The process of running an OpenFOAM simulation starts with creating a .STL file of the foil. This file can then be rotated to whatever angles of attack desired for simulating. These rotated foils are then able to be placed in the triSurface folder and simulated one by one. The commands for running the HiCaT simulations in OpenFOAM are as follows:

1. blockMesh: globally meshes the test section.
2. surfaceFeatureExtract: creates the eMesh file.
3. DecomposePar: breaks down mesh for snappyHexMesh.
4. snappyHexMesh: merges foil mesh with global mesh.
5. reconstructParMesh: puts decomposed mesh back together.
6. DecomposeParMesh: decomposes mesh once again, but this time to run simpleFoam.
7. foamJob: runs simpleFoam in parallel.
8. reconstructParMesh: reconstructs mesh for final visualization.
9. Vorticity: calculates vorticity for later visualization.

When it comes to computational work processing speed becomes a major factor. In the beginning computational work was performed on a personal laptop running on one processor, these simulations took a full 24 hours to converge. The power of running multiple processors in parallel allowed for the simulations to converge overnight in a time span of about 12 hours. Being limited to 4 processors on a personal computer forced the movement to a higher processing workstation. The workstation used was the core-simulator located in the Chase engineering building. This computer has 8 processors and allowed for a simulation to converge in about 4-5 hours. The option of using OpenFOAM on the mechanical engineering server at UNH (Mech-3) is now available with the capability of using 12 processors and 96 GB of ram.

In order for OpenFOAM to be applied to the design of a new wingtip the numerical testbed first needed to be validated. To do this numerical simulations were created for the endcap, general foil, and split tip foil. These results could then be compared to the experimental results obtained in the HiCaT facility and used to validate the numerical test bed. These graphs can be seen in results section 5, Figures 20-22.

Once the experimental results were validated numerically this testbed could be applied to the design of future wingtips. Since the split tip has a complex design, is difficult to manufacture and could be prone to biofouling it was decided to take a more simplistic approach which is cheaper to manufacture and less prone to biofouling. For this design the twist parameter of the wingtip was

varied from 0-6 degrees. The idea behind this was to balance the pressure distribution at the tip of the foil reducing induced drag at the cost of pressure drag. The results of the design iteration are shown below in Figure 4.

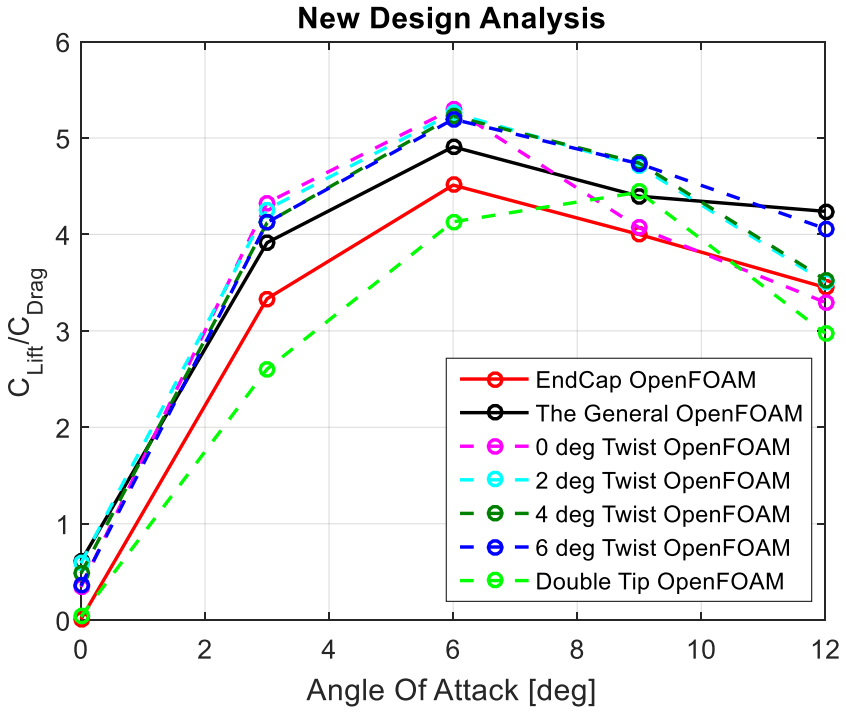

Figure 4: Computational analysis of the Twist Tip.

By looking at the numerical results obtained it can be seen that even at 0 degree twist angle this winglet has a higher C_{lift}/C_{drag} peak than both the general foil and the endcap. After 6 degrees induced drag becomes dominant and the overall performance of these foils begins to drop. This is the point where the twist tip helps the overall performance of the foil. The more twist that is applied the better it performs at higher angles of attack.

4 Experimental Analysis

4.1 High-Speed Cavitation Tunnel (HiCaT)

Cavitation studies were performed in the High-Speed Cavitation Tunnel (HiCaT), shown in Figure 5. The HiCaT was designed to allow for fundamental studies in of high-speed water flows of up to 17 m/s for various applications such as conventional hydropower, marine renewable energy, pumps, marine vehicles, drag reduction and industrial processes. It has the ability to control inside pressure and speed of the fluid independently. The hydrofoils can be accommodated in the 6" wide x 6" high x 36" long test section. A force balance is located behind the test section and allows for attainting the lift and drag forces on the hydrofoil for varying angles of attack, as well as pressure on the surface of the foil at given locations.

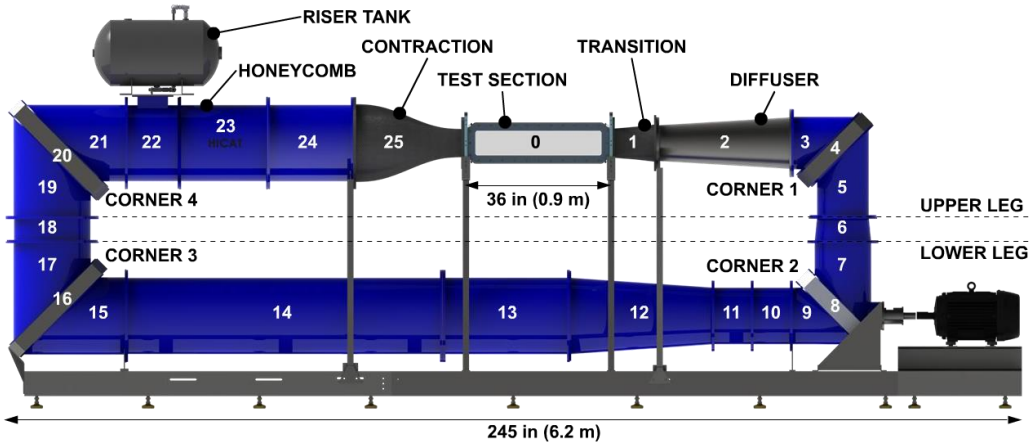

Figure 5: HiCaT located in Chase Ocean Engineering Laboratory.

Before performing an experiment, the test section must be taken apart and the force balance must be calibrated. The calibrating procedure is describe in Section 4.2.

4.2 Tunnel Calibration

1. Boot up computer and open LabView.
2. Open: balance_and_pressure_new_file_writing.vi this will be used to display and record the experimental data for calibration the user interface is shown in Figure 6.

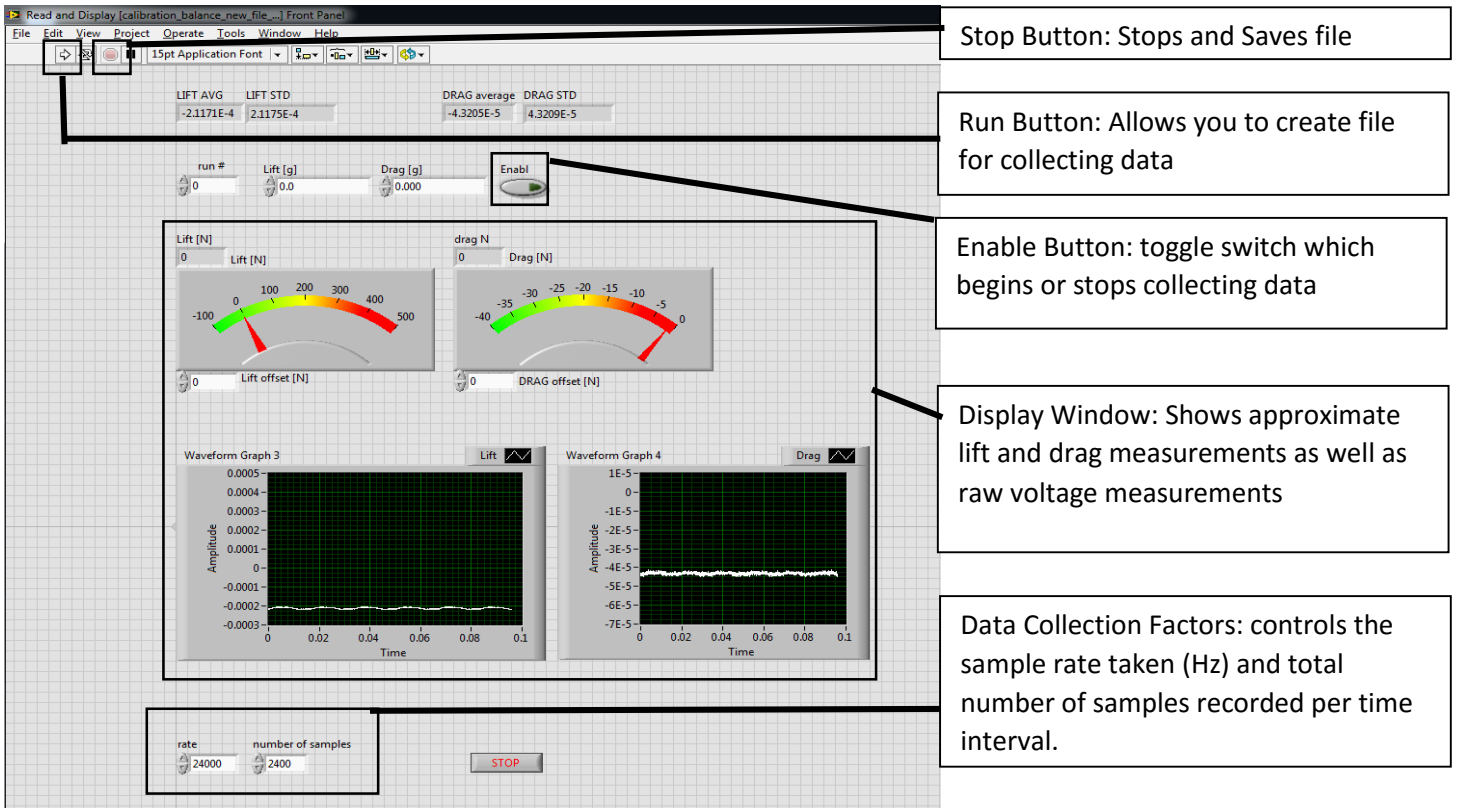

Figure 6: LabView user interface.

3. On the test section of the HiCaT tunnel remove the front acrylic window:
    a. Remove all bolts holding the window in.
    b. Remove 3 bolts on the side of the window blocking the window from being removed.
    c. Tap washers in between window and metal across top to begin separation.
    d. Once the window is separated evenly across the top use a flathead screwdriver to gently pry window out.
    e. Once window gap is large enough insert larger pry bar and pry top and bottom out evenly until window comes out.
    f. Place window in black cabinet.
4. Remove bottom acrylic window:
    a. Remove all bolts holding window in.
    b. Remove 3 bolts blocking window from being removed (shown below in figure X)
    c. Using rubber mallet tap back and forth on inside of the window.
    d. Place window and gasket in black cabinet (gasket may be stuck to test section).

5. Remove rod connecting wing to force balance:
    a. Loosen bottom two bolts holding rod in place (behind drag plate).
    b. Slide rod out and place somewhere safe.
6. Remove 4 bolts holding foil to rod.
7. Bolt calibrating plate in place of foil.
8. Reinstall rod and tighten down bolts (use digital level to make sure that it is level).

Figure 7: Digital level set up.

9. Bolt pulley into place far from calibrating plate for best accuracy.
10. Get bucket and string ready and record mass of bucket.
11. On the computer hit the run button in Labview and name file
12. With nothing connected to the calibration plate hit the enable button on the Labview to allow it to collect and average output voltages from the strain gauges.
13. Attach the bucket to the calibration plate wrapping the string around the pulley.

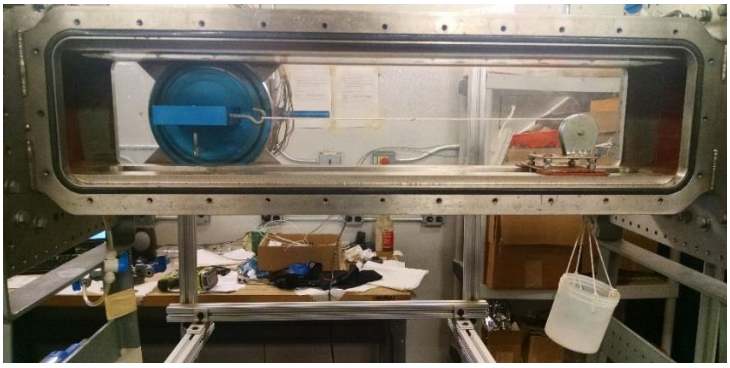

Figure 8: Mass-string pulley system used for calibration.

14. Input the mass into Labview, increase the run number by 1 and hit enable again.
15. Add masses in 200g increments to bucket recording results until 1800g is reached.

4.3 Dynamic Response

As part of the experimental studies, the effect of vortex shedding was recreated by simulating a dynamic response of a foil. Vortex shedding occurs when a cavity forms on one side of the foil, sheds away and reforms again. This occurs at frequencies of 40-60 Hz, causing oscillations to the system. The phenomenon can be seen in Figure 9 below.

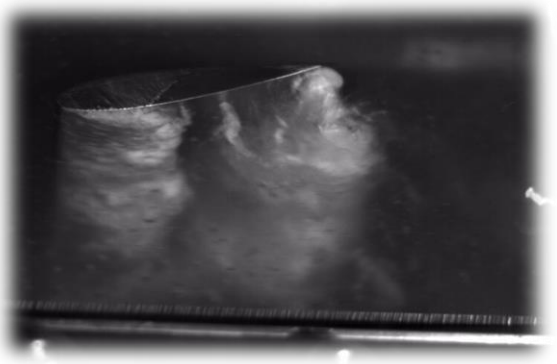

Figure 9: Formation and shedding of cavitation.

The force balance on the HiCaT tunnel can be seen in Figure 10. The force was applied to the tip of the test object. The rigid components of the force balance were the test object, the seal, the rod and the drag plates.

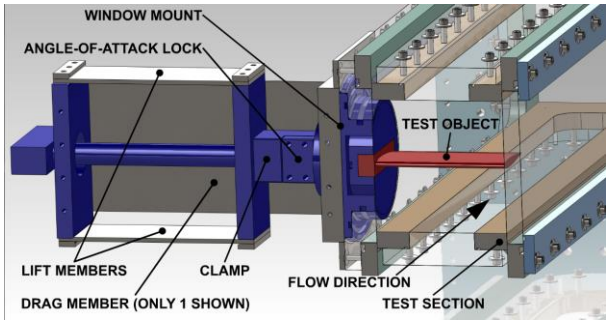

Figure 10: Force balance in the HiCaT tunnel.

The seal is located inside the window mount component and an image of the balance with and without seal can be seen in Figure 11.

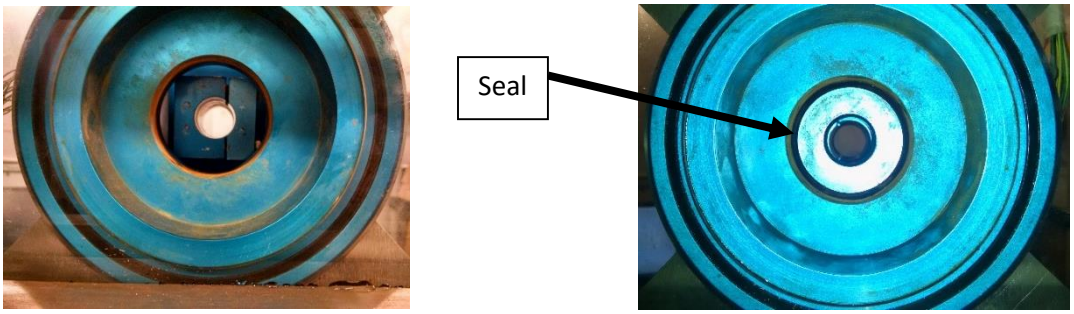

Figure 11: Drag force balance with the seal (right) and without (left).

A number of assumptions were made before modelling the system. First, although the experiment was performed with and without seal, theoretical calculations were only made without the seal. The drag plates on the force balance were modelled as cantilever beams and were assumed to provide damping. The system was modelled as a mechanical mass-spring-damper system and the schematics of the model can be seen in Figure 12.

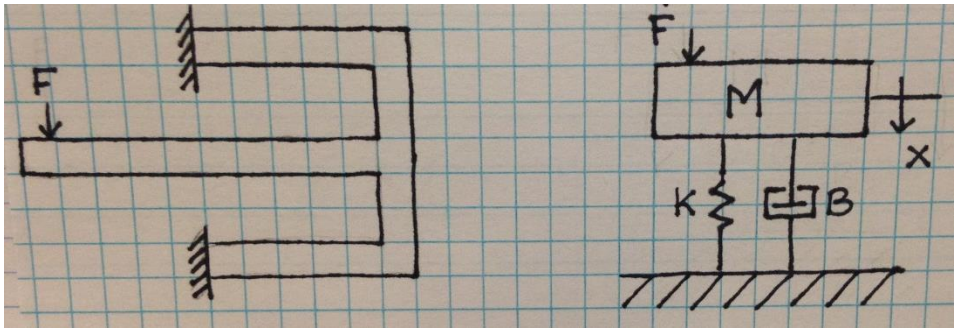

Figure 12: Mechanical Second Order System schematics.

The system can be represented mathematically through the following equation of motion

$$M\ddot{x} + B\dot{x} + kx = k_s F \tag{1}$$

where M is the equivalent mass of the system, B is the damping coefficient, k is the spring coefficient, k_s is the gain, and F is the step input. A derived transfer function for the system is

$$\frac{X(s)}{F(s)} = \frac{k_s}{{}^{M}/_{k}\, s^2 + {}^{B}/_{k}\, s + 1} \tag{2}$$

The stainless steel drag plate was modelled as a cantilever beam and the spring coefficient of each beam was calculated using the following equation.

$$k_{Theoretical} = \frac{F}{\delta} = \frac{2Ewt^3}{5L^3} \tag{3}$$

Where F is the drag force, δ is the displacement at the location of the strain gauge, E is the Young's modulus, t is the beam thickness, w is the width, and L is the beam length. (Note: for derivation look appendix).

The system parameters are shown in Table 1.

Mass (M)	9.26 kg
Young's Modulus (E)	203 GPa
Drag Plate Width (w)	0.15 m
Drag Plate Thickness (t)	0.0016 m
Drag Plate Length (L)	0.30 m
Spring Coefficient ($k_{Theoretical}$)	3608.4 N/m

Table 1: System parameters.

The dynamic response of the drag force sensor was analyzed in the HiCaT tunnel. This was done with and without the inner seal in order to discover seals effect on the sensor. To simulate the dynamic response an analytical and experimental analysis has been performed by placing a known weight in a bucket and cutting the string, simulating a fully reversed load on the sensor. This procedure captures real time data of the force sensor and saves the data in .lvm format for later analysis. The procedure used was as follows:

1. Open: balance_and_pressure_new_file_writing_continuous.vi this will be used to display and record real time experimental data for analysis.
2. Attach the bucket to the calibration plate wrapping the string around the pulley and place the desired weight in the bucket (500, 1000. 1400 were used)
3. Click run in labview then allow a second of data collection and cut the string holding the bucket (make sure you catch the falling bucket).

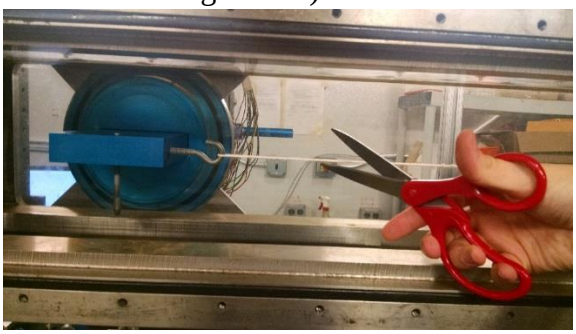

Figure 13: Mass-string pulley system simulating a fully reversed load on the sensor.

4. View the results and make sure that the response was captured.

To analyze the force sensor without the seal the seal must first be removed. To do this the following procedure is followed.

1. Remove the entire drag sensor from the tunnel. To do this remove the top and bottom 4 bolts attaching the sensor to the test section shown in Figure 14.

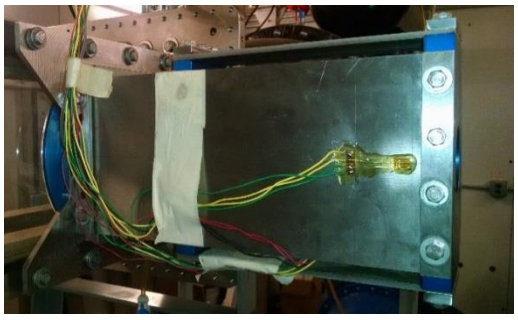

Figure 14: Drag sensor on the tunnel.

2. Once the bolts are removed the sensor can be separated.
3. To remove the seal unbolt the outer ring of Alan bolts and take the inner ring and seal out.
4. Rebolt the outer ring in and reassemble the sensor.

The calibration curve for the force balance without and with the seal can be seen in Figure 15, respectively. The force balance sensitivity with the seal was determined to be 616 kN/V and the sensitivity without the seal was determined to be 425 kN/V. The sensitivity difference was determined to be 31% and was calculated using the following equation

$$\% \, Difference = \frac{S_S - S_{NS}}{S_S} \tag{4}$$

where S_S is the sensitivity of the balance with the seal and S_{NS} is the sensitivity of the balance without the seal.

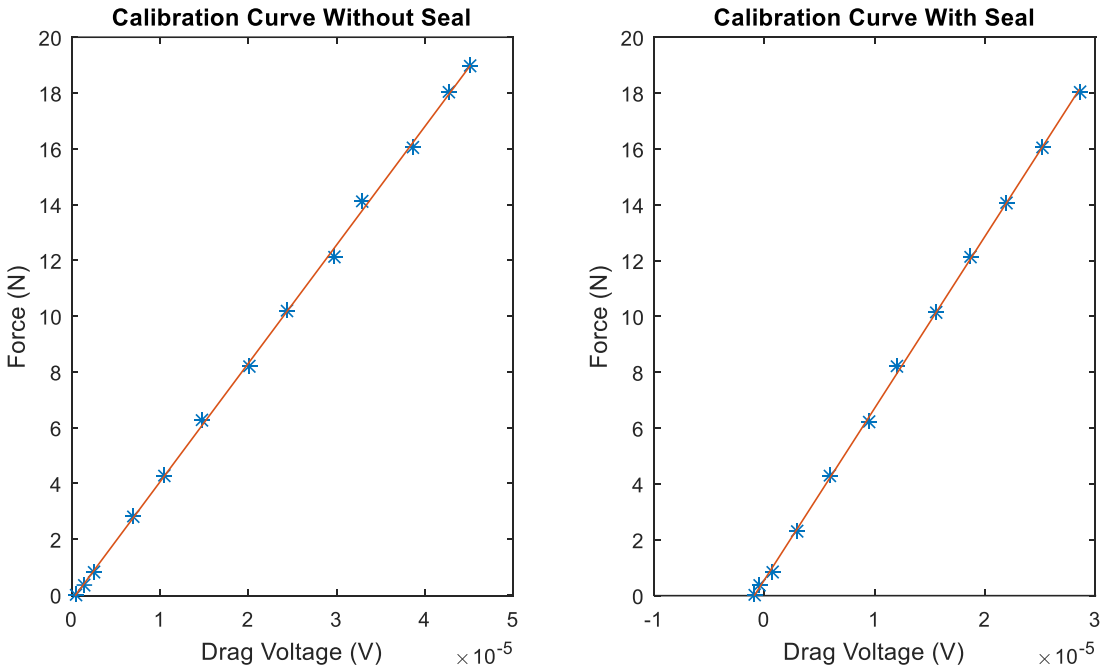

Figure 15: Force balance curve with seal (right) and without seal (left).

Figure 16 shows the dynamic response of the system with and without seal with a known mass of 500 g. Using the logarithmic decrement method natural frequency and damping ratio were determined. The calculated values can be seen in Table 2.

	Seal	**No Seal**
$\boldsymbol{\omega_n}$	19.3 Hz	15.7 Hz
$\boldsymbol{\xi}$	0.0166	0.0051
B	6 kg/s	1.5 kg/s

Table 2: Experimental natural frequency and damping ratio values.

The standard equation for a second order system is shown in Equation 5

$$\frac{X(s)}{F(s)} = \frac{k_s}{\frac{1}{\omega_n^2}s^2 + \frac{2\xi}{\omega_n}s + 1} \tag{5}$$

Combining equations 2 and 5 an equation for the system's damping coefficient was derived and is shown below

$$B = k_{Theoretical}\frac{2\xi}{\omega_n} \tag{6}$$

The value of the damping coefficient was determined to be 1.87 kg/s.

A theoretical value of the natural frequency has been calculated for comparison using the following equation

$$\omega_{n,Theoretical} = \sqrt{\frac{k_{Theoretical}}{M}} \tag{7}$$

The value of the theoretical natural frequency was determined to be 19.74 Hz. The percentage error between the theoretical and experimental value was 20.3 %.

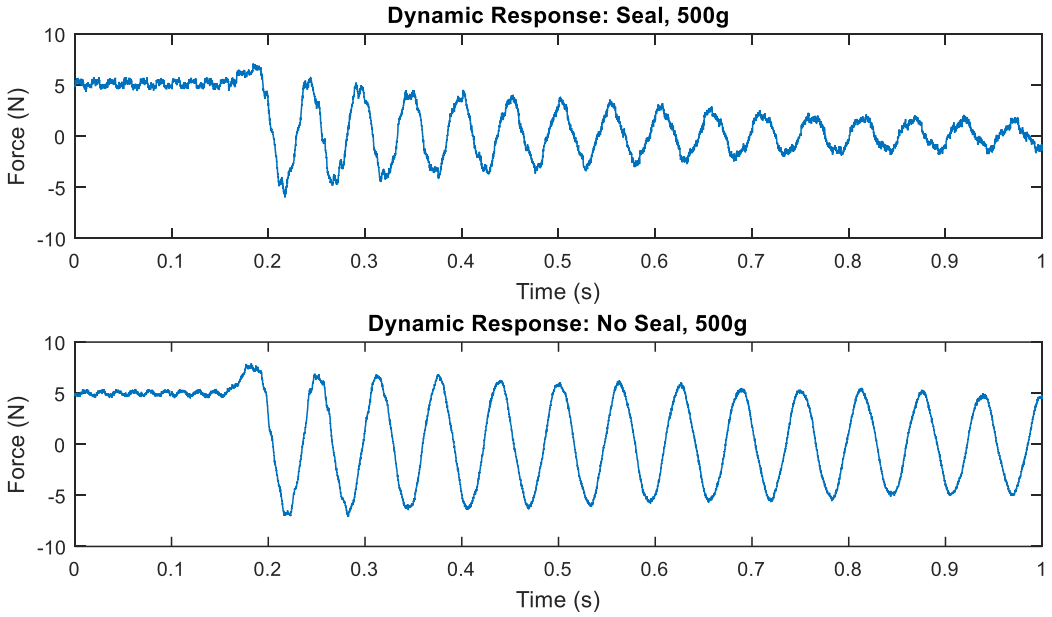

Figure 16: Dynamic response of the system with and without seal with a known mass of 500 g.

The dynamic response of the balance with the seal has notably less oscillations from which it can be concluded that the seal provides additional damping to the system. The natural frequency is much larger with the seal in. The percent overshoot is greater when the seal was removed and the damping ratio increased significantly.

Using the natural damping frequency and damping ratio, response time, settling time and frequency of oscillations were calculated using equations 8, 9 and 10 respectively.

$$T_{ResponseTime} = \frac{1}{\omega_n \xi} \tag{8}$$

$$T_{SettlingTime} = \frac{4}{\omega_n \xi} \tag{9}$$

$$f_{Oscillation} = \frac{1}{t_2 - t_1} \tag{10}$$

The calculations have been performed for the seal and no seal case and the results can be seen in Table 3 below.

	Seal	No Seal	% Difference
Response Time	0.50s	1.97s	294
Settling Time	2.0s	7.9s	295
Frequency	19.3 Hz	15.7 Hz	18.7

Table 3: Experimental Response time, settling time and frequency of oscillation.

A frequency response has been generated for the force balance without the seal and can be seen in Figure 17 below. The sensor is a low-pass filter which means that the dynamic frequencies lower than the break frequency can be measured with this sensor. Any frequencies after this point will be attenuated. The frequency of vortex shedding is significantly higher than the break frequency of the system and therefore cannot be measured.

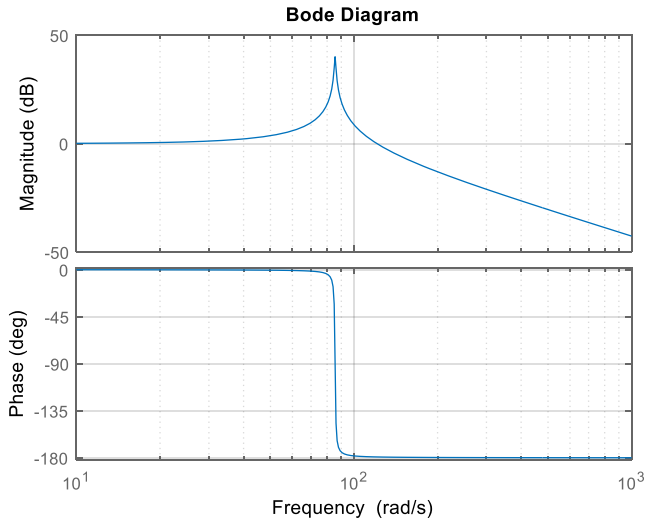

Figure 17: Frequency response Bode plot of the system.

An experimental spring coefficient for the force balance without the seal has been calculated using the following equation

$$k_{NoSeal} = M\left(\frac{\omega_{n,NoSeal}}{2\pi}\right)^2 \tag{11}$$

where $\omega_{n,NoSeal}$ is the natural frequency of the system without the seal. The value of the spring coefficient without the seal was determined to be 3880 N/m. This yields a percentage error of

7.5%. To investigate the effects of the seal a spring constant for the system has been calculated using the following equation

$$k_{Seal} = M\left(\frac{\omega_{n,Seal}}{2\pi}\right)^2 \tag{12}$$

where and $\omega_{n,Seal}$ is the natural frequency of the system with the seal. The value of the spring coefficient with the seal was 67618 N/m.

The dynamic response was also analyzed in the lift direction. It was determined that the lift force response time was 0.23 s and the lift force frequency of oscillation 54 Hz, which means that the time response of the lift sensor is quick enough to measure vortex shedding.

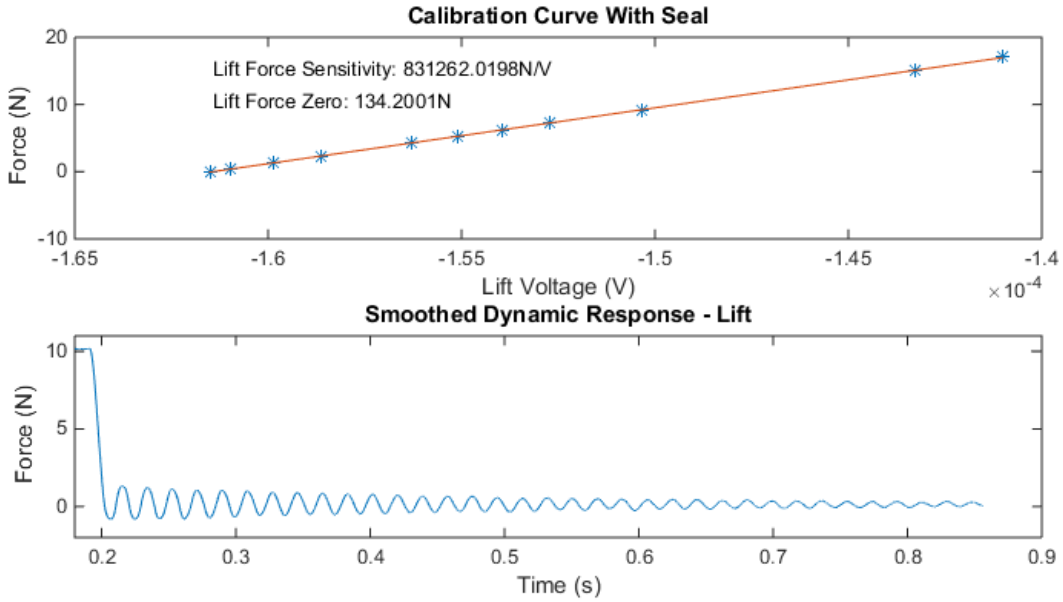

Figure 18: Lift dynamic response of the system.

4.4 Drag Plate Studies

In addition, in order to more accurately capture the drag forces on the hydrofoil, new drag plate which was 0.02" thinner than the old one was manufactured and installed onto the force balance. The tunnel was re-calibrated and the experiments for the existing foils were repeated.

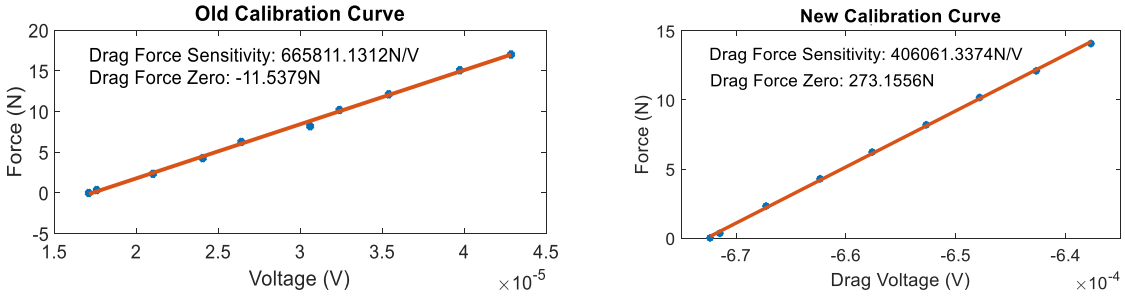

Figure 19: Force balance calibration with the old drag plate (left) and the new drag plate (right).

As seen in Figure 19, replacing the drag plate showed an increase in the sensitivity and overall improvement in the resolution. Sensitivity went from 665,811 N/V to 406,061 N/V, making it 34% more sensitive. Replacing the drag plate had a negative effect on the dynamic response, however the new dynamic response was not tested.

5 Results

Shown in Figures 20, 21 and 22 is the numerical and experimental comparison of the lift and drag coefficients as a function of the angle of attack for the end cap, the general foil, and the split tip, respectively.

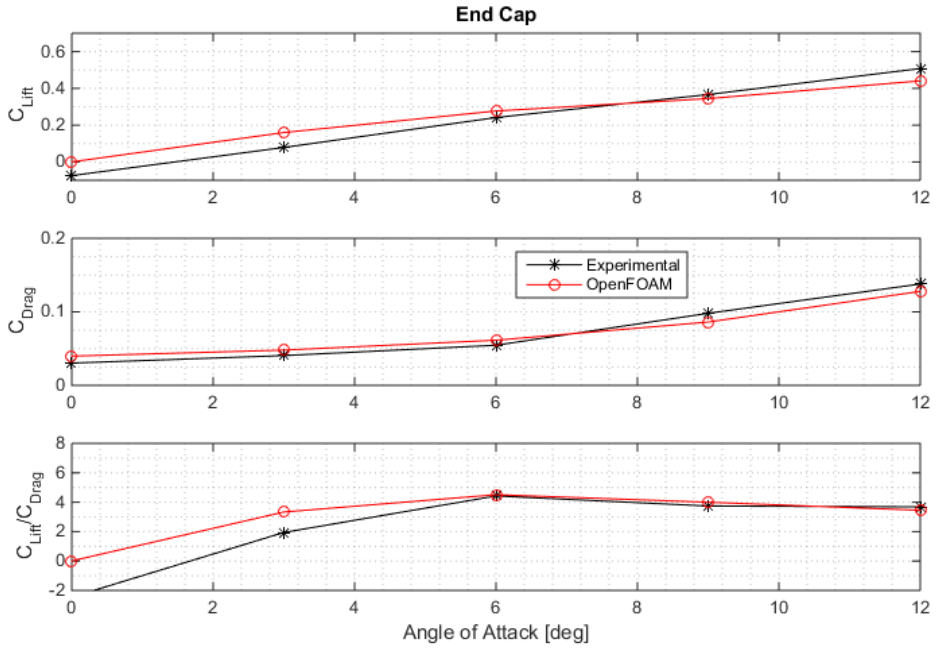

Figure 20: The numerical and experimental comparison of lift and drag coefficients of the end cap as a function of the angle of attack.

The third subplot of each of the figures shows the ratio of the two coefficients which represents the overall performance of each wingtip. In all three cases, the computation data matched closely with the experimental. The overall performance of the general foil was significantly higher than that of the end cap foil. Both the experimental and numerical data suggest that the optimal angle of attack for the general foil is 6°. In the case of the split tip foil, the experimental data yields slightly better results than the computational. Experimentally, the optimal angle of attack for the split tip is 12°. The overall performance of the split tip at the optimal angle is higher than that of the general foil, and significantly higher than that of the end cap. The numerical data obtained through OpenFOAM was least accurate for the split tip. This is due to the complex geometry of the split tip.

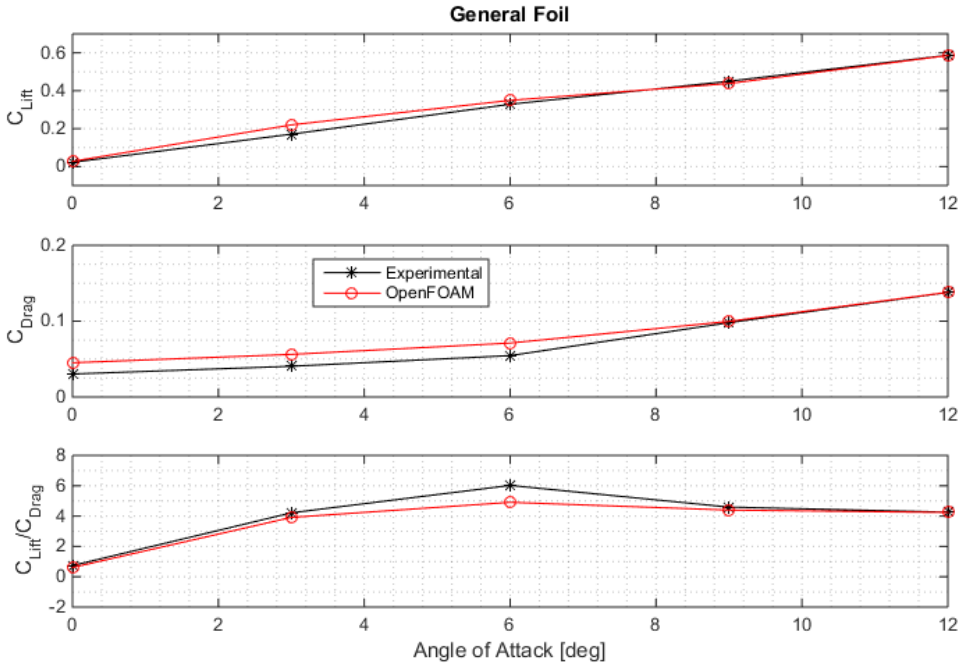

Figure 21: The numerical and experimental comparison of lift and drag coefficients of the general foil as a function of the angle of attack.

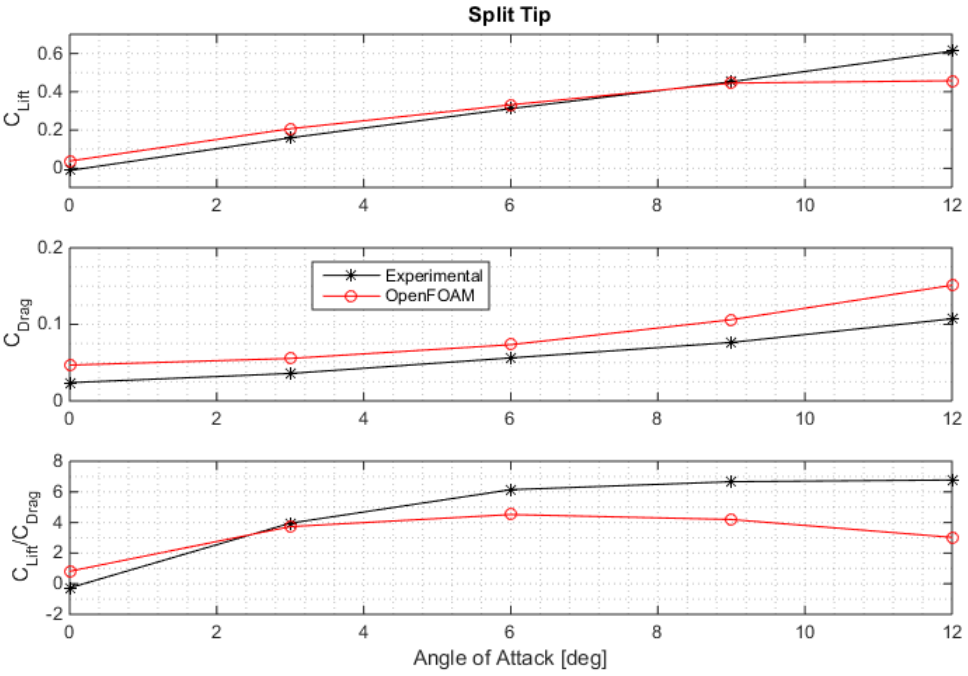

Figure 22: The numerical and experimental comparison of lift and drag coefficients of the split tip as a function of the angle of attack.

6 Conclusions

In conclusion, the sensitivity of the force balance is significantly different with and without the seal. The sensitivity with the seal was 616 kN/V and the sensitivity without the seal was 425 kN/V yielding a percentage difference of 31%. The natural frequency of the balance with and without the seal was 19.3 Hz and 15.7 Hz, respectively. The theoretical natural frequency was 19.74 Hz and it was calculated neglecting the seal. The percent error between the theoretical and experimental values for the balance with no seal was 3.7 %. An experimental spring coefficient was determined to be 3880 N/m compared to the theoretical value of 3608.4 N/m, yielding a percent error of 7.5 %.

The time response of the balance without the seal was 1.97 s, which is significantly slower than that 0.5 s for the balance with the seal. Similarly, the settling time of force balance without the seal, 7.9 s was longer than that of the balance with the seal, 2.0 s. The frequency of oscillations for the balance with and without the seal was 19.3 Hz and 15.7 Hz, respectively. Although the time response of the balance is quick, it is not quick enough to accurately measure vortex shedding which occurs at frequencies of 40-60 Hz.

The new drag plate is performing more consistently and accurately than the old one. Although replacing it had a negative effect on the dynamic response of the system, the new plate is over 30 % more sensitive and producing significantly better experimental results.

The experimental and the numerical data for the end cap foil, the general foil, and the split tip matched very closely. Both, the general foil and the split tip performed better numerically and experimentally compared to the end cap foil. The optimal angle of attack for the general foil and endcap foil is 6 degrees and the optimal angle of attack for the split tip is 12 degrees. The overall performance of the split tip at the optimal angle is higher than that of the general foil, and significantly higher than that of the end cap.

The new design was a modification of the general foil which is easy to manufacture and not as prone to bio-fouling. The wingtip was tapered in order to decrease the friction drag. The twist angle was adjusted from 0- 6 degrees in intervals of 2 degrees. The twist tip was simulated for 0 -12 degrees angles of attack for each iteration of the twist angle. After the angle of attack exceeded 6 degrees induced drag became dominant and the overall performance of these foils begun to drop. At that point the twist tip helps the overall performance of the foil. The more twist that is applied the better it performs at higher angles of attack.

7 Future Development

- Run simulations on 12 processors through the mechanical engineering server and look into the possibility of GPU processing.
- Split the numerical testbed into multiple sections and use a stacked mesh towards the foil to increase mesh density near the foil allowing for better resolution of tip vortices.
- Use DC power supply when the dynamic response is of interest in order to avoid the 60 Hz noise of the NI power supply.
- Look into other classical wingtip parameters in order to optimize general foil profile.
- Investigate the dynamic response of the new drag plate.
- Investigate the possibility of cross-communication between the lift plate and the new, thinner drag plate.

8 References

[1] Brindley, John, Jesse Shull, and Ian Gagnon. ‘’*Developing Hydrokinetic Wingtip Devices’’. 2014*. Web

[2] J. Johansen and N.N. Sorensen, ‘*’Aerodynamic investigation of Winglets on Wind Turbine Blades using CFD*’’, Riso-R-1543 (EN), Riso National Laboratory, Roskilde, February, 2006.

[3] Nedyalkov, Ivaylo. *Design of Contraction, Test Section, abd Diffuser for a High-Speed Water Tunnel*. Thesis, Chalmers University of Technology. Gothenburg, Sweden 2012.

[4] Therrien, Ryan, Spencer Roux, and Ben Comtois.*’’Design of High Speed Water Tunnel Force Balance & Testing of High Performance Hydrofoils for Marine Hydrokinetic Turbines*.’’ *2012*. Web.

9 Acknowledgements

Advisors: Martin Wosnik, Ivaylo Nedyalkov

Machining: Scott Campbell, Sheldon Parent

Funding: This work is the result of research sponsored in part by the New Hampshire Sea Grant College Program through NOAA grant # NA10OAR4170082, and the UNH Marine Program.

Other: John Brindley, Jesse Shull, Alexander Larson

10 Appendix

10.1 OpenFOAM Figures

End Cap:

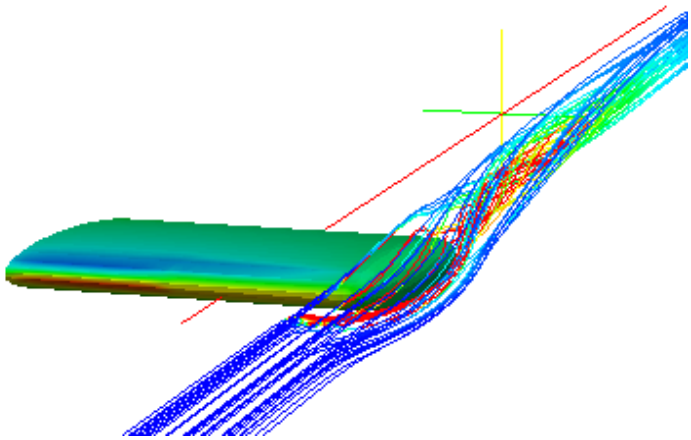

Figure 23: OpenFOAM image showing vorticity in the streamlines and the pressure distribution across the End Cap Foil.

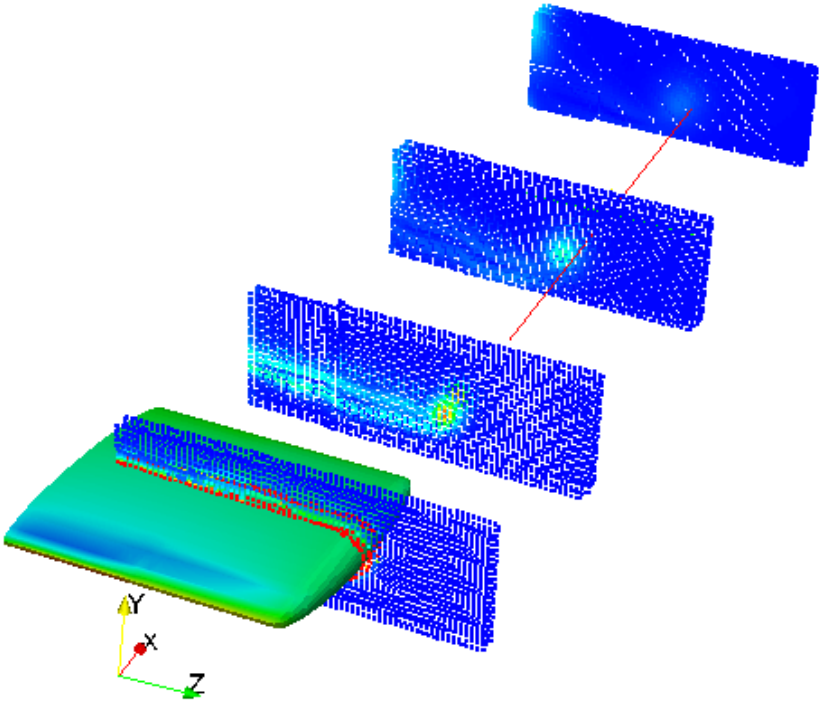

Figure 24: OpenFOAM image showing vorticity in the cross sections and the pressure distribution across the End Cap Foil.

General Foil:

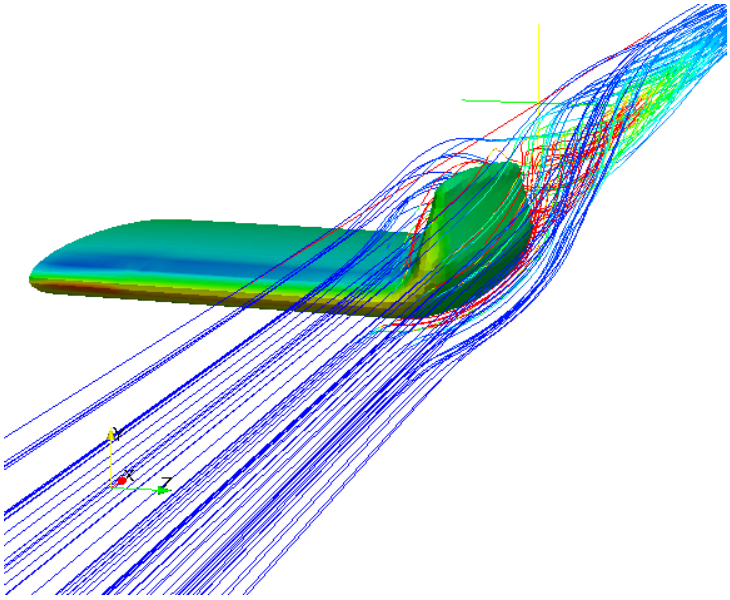

Figure 25: OpenFOAM image showing vorticity in the streamlines and the pressure distribution across the General Foil.

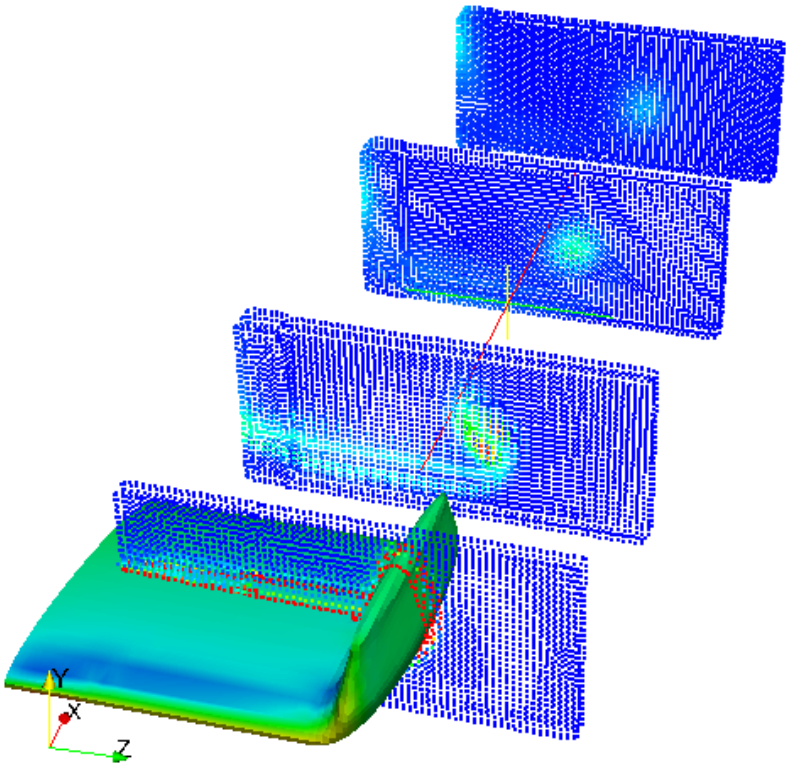

Figure 26: OpenFOAM image showing vorticity in the cross sections and the pressure distribution across the General Foil.

Split Tip:

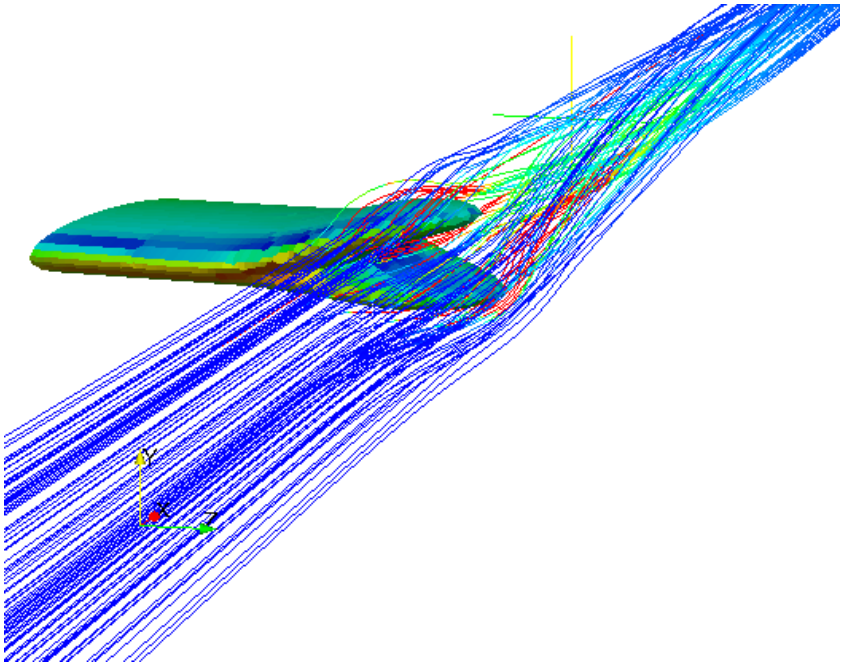

Figure 27: OpenFOAM image showing vorticity in the streamlines and the pressure distribution across the Split Tip.

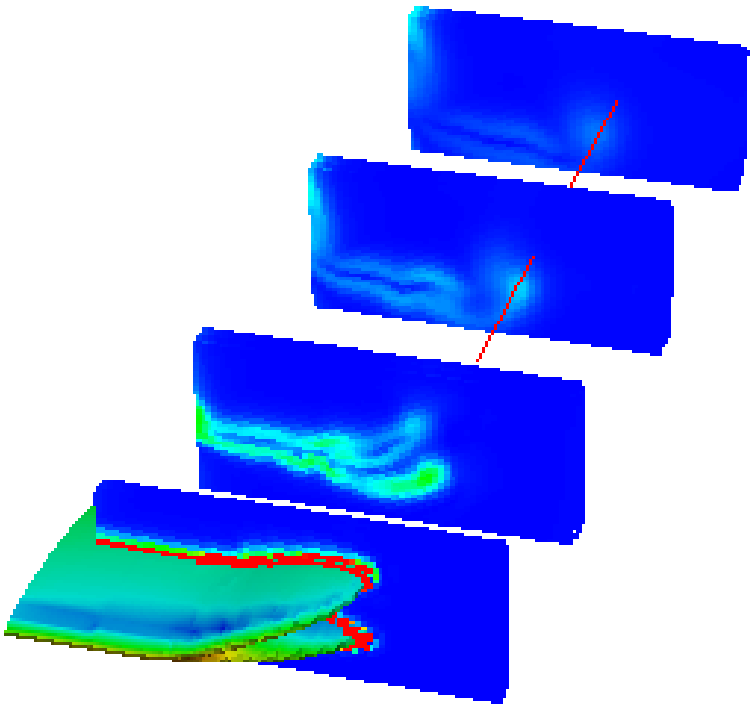

Figure 28: OpenFOAM image showing vorticity in the cross sections and the pressure distribution across the Split Tip.

Twist Tip:

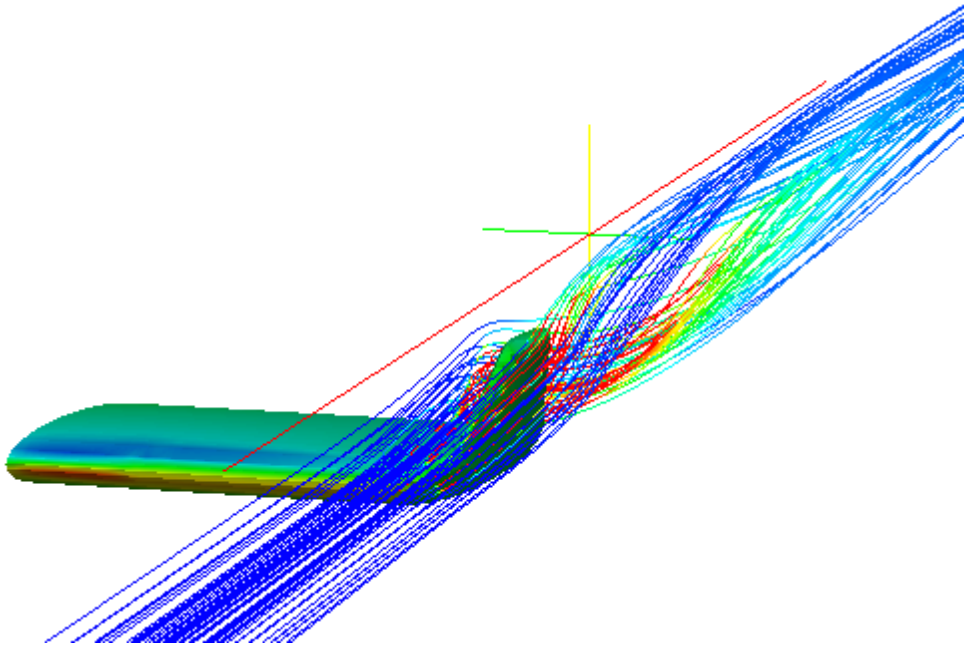

Figure 29: OpenFOAM image showing vorticity in the streamlines and the pressure distribution across the Twist Tip.

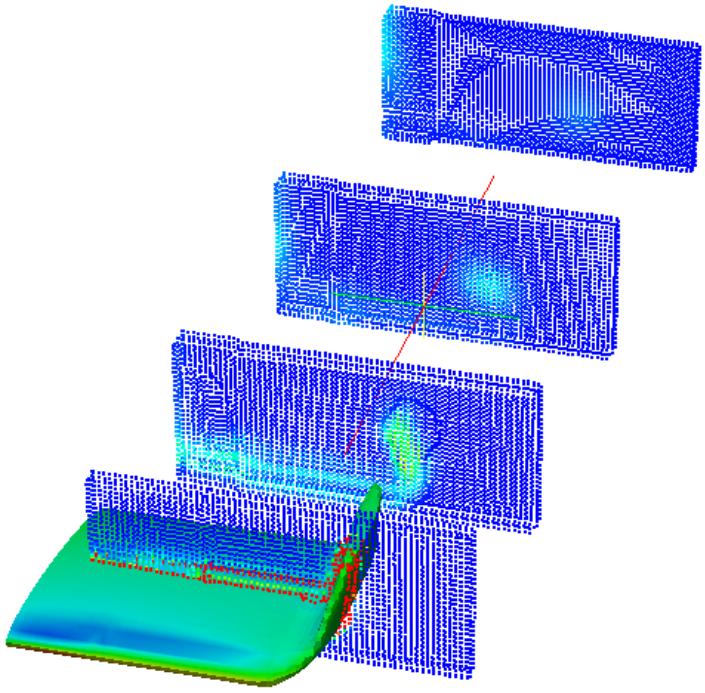

Figure 30: OpenFOAM image showing vorticity in the cross sections and the pressure distribution across the Twist Tip.

10.2 MATLAB Code

```
%% Loading Data

clear all
close all
clc

% S=with seal, #=amount of weight added
%seal 500g added
n=24;
sldata1=importdata('2016_Feb12_LiftDynamicTest1kg.lvm','\t',n);
s2=sldata1.data;
t_s=s2(:,1); %time
vdrag_s=s2(:,6).*1000; %drag voltage
vlift_s=s2(:,5).*1000; %drag voltage

n1=24;
sldata1=importdata('2016_Feb12_LiftCali.lvm','\t',n1);
s1=sldata1.data;
m1=s1(:,3); %mass in kilograms
n=s1(:,2).*1000; %data number
vdrag1=s1(:,7).*1000; %drag voltage
vlift1=s1(:,5).*1000; %drag voltage
%% Data Analysis
%calibrating scale with seal
cc=1;
m(1)=m1(1);
vdrag(1)=vdrag1(1);
vlift(1)=vlift1(1);
for i=2:length(m1)
    if n(i)>n(i-1)
        cc=cc+1;
        m(cc)=m1(i);
        vdrag(cc)=vdrag1(i);
        vlift(cc)=vlift1(i);
    end
end

%erasing bad points
%m=[m5(1:6),m5(8:length(m5)-1)];
%vdrag=[vdrag5(1:6),vdrag5(8:length(vdrag5)-1)];

F=m.*9.81;
[ m_s, b_s ] = Sensativity( vlift, F); %m11 is the sensativity of the drag
balance in N/V
Fnew=m_s.*vlift+b_s;
fprintf(['\nLift Force Sensativity With Seal: ' num2str(m_s) 'N/V\n'])
fprintf(['Lift Force Zero With Seal: ' num2str(b_s) 'N\n'])
figure
plot(vlift,F,'*',vlift,Fnew)
ylabel('Force (N)')
xlabel('Lift Voltage (V)')
title('Calibration Curve With Seal')
text(vlift(1),F(length(F)),['Lift Force Sensativity: ' num2str(m_s) 'N/V'])
text(vlift(1),F(length(F)-1),['Lift Force Zero: ' num2str(b_s) 'N'])
```

```
%% Dynamic Component
%truncating beginning and end of each data set, converting to newtons, and
%smoothing the data
smooth_num=165;
%seal data
SettlingValue=1.4;
figure
plot(t_s(smooth_num:2*smooth_num),vlift_s(smooth_num:2*smooth_num))
[ tnew_s_500,Flift_s  ] = trunc( t_s, vlift_s, m_s, b_s
,smooth_num,SettlingValue);

%%
figure
subplot(2,1,2)
plot(tnew_s_500,Flift_s)
ylabel('Force (N)')
xlabel('Time (s)')
title('Smoothed Dynamic Response - Lift')
axis([0.18 0.9 -2 11])
subplot(2,1,1)
plot(vlift,F,'*',vlift,Fnew)
ylabel('Force (N)')
xlabel('Lift Voltage (V)')
title('Calibration Curve With Seal')
text(vlift(1),F(length(F)),['Lift Force Sensitivity: ' num2str(m_s) 'N/V'])
text(vlift(1),F(length(F)-1),['Lift Force Zero: ' num2str(b_s) 'N'])

%fprintf(2,'Dynamic Response Attempt 1 FAILED\n')

%% Plotting all of the dynamic responses together
% figure
% subplot(3,2,1)
% plot(tnew_s_500,Flift_s)
% xlim([0 1])
% ylabel('Force (N)')
% xlabel('Time (s)')
% title('Dynamic Response: Seal 500g')
% hold on
%
% subplot(3,2,2)
% title('Dynamic Response of Drag Force Balance')
% plot(tnew_ns_500,Fdrag_ns_500)
% xlim([0 1])
% title('Dynamic Response:No Seal 500g')
% ylabel('Force (N)')
% xlabel('Time (s)')
% hold on
%
% subplot(3,2,3)
% plot(tnew_s_1000,Fdrag_s_1000)
% xlim([0 1])
% title('Dynamic Response: Seal 1000g')
% ylabel('Force (N)')
% xlabel('Time (s)')
% hold on
```

```
%
% subplot(3,2,4)
% plot(tnew_ns_1000,Fdrag_ns_1000)
% ylabel('Force (N)')
% title('Dynamic Response:No Seal 1000g')
% xlabel('Time (s)')
% xlim([0 1])
% hold on
%
% subplot(3,2,5)
% plot(tnew_s_1400,Fdrag_s_1400)
% title('Dynamic Response:Seal 1400g')
% ylabel('Force (N)')
% xlabel('Time (s)')
% xlim([0 1])
% hold on
%
% subplot(3,2,6)
% plot(tnew_ns_1400,Fdrag_ns_1400)
% title('Dynamic Response:No Seal 1400g')
% ylabel('Force (N)')
% xlim([0 1])
% xlabel('Time (s)')
% hold on

%% Determining the time response of the system

span_s=1;
window_s=ones(span_s,1)/span_s;
smoothdata_s=conv(Flift_s,window_s,'same');
theshold=0.1;
[pks,dep,pidx,didx]=peakdet(smoothdata_s,theshold,'theshold');
peaks_s=pks;
peakloc_s=pidx;



figure
plot(tnew_s_500,Flift_s,'.')
hold on
plot(tnew_s_500(peakloc_s),peaks_s,'d',tnew_s_500(didx),dep,'d')
hold off

f=1/(tnew_s_500(peakloc_s(3))-tnew_s_500(peakloc_s(2)));
Wd=(2*pi).*(f);
delta = (1/3)*log((peaks_s(2))/(peaks_s(5)));
zeta= (1)/sqrt(1+(((2*pi)/delta).^2));
Wn= Wd/(sqrt(1-(zeta.^2)));

Tst=1/(Wn*zeta); %Response time of the sensor (s)

tst=1/40; %period of vortex shedding input (s)

fprintf(['\nLift Force Response Time: ' num2str(Tst) 's'])
fprintf(['\nLift Force Frequency of Oscillation: ' num2str(f) 'Hz'])
```

```
PO_theory=100.*exp(-zeta*pi/(sqrt(1-(zeta^2))));
PO_exp=100*(-dep(1)/pks(1));

error=-((tst-Tst)/tst)*100;
fprintf(['\nLift Force Time Response Error: ' num2str(error) '%\n'])
% %% Determining the time response of the system With Seal
%
% span_s=1;
% window_s=ones(span_s,1)/span_s;
% smoothdata_s=conv(Flift_s,window_s,'same');
% theshold=0.1;
% [pks,dep,pidx,didx]=peakdet(smoothdata_s,theshold,'theshold');
% peaks_s=pks;
% peakloc_s=pidx;
%
% figure
% plot(tnew_s_500,Flift_s,'.')
% hold on
% plot(tnew_s_500(peakloc_s),peaks_s,'d')
% hold off
%
% f=1/(tnew_s_500(peakloc_s(3))-tnew_s_500(peakloc_s(2)));
% Wd=(2*pi).*(f);
% delta = (1/3)*log((peaks_s(2))/(peaks_s(5)));
% zeta= (1)/sqrt(1+(((2*pi)/delta).^2));
% Wn= Wd/(sqrt(1-(zeta.^2)));
%
% Tst=1/(Wn*zeta); %Response time of the sensor (s)
% Tsst=4*Tst;
% tst=1/40; %period of vortex shedding input (s)
%
% fprintf(['\nDrag Force Response Time: ' num2str(Tst) 's'])
% fprintf(['\nDrag Force Frequency of Oscillation: ' num2str(f) 'Hz'])
%
%
% error=-((tst-Tst)/tst)*100;
% fprintf(['\nDrag Force Time Response Error: ' num2str(error) '% \n'])
%
% PO_s_theory=100.*exp(-zeta*pi/(sqrt(1-(zeta^2))));
% PO_s_exp=100*(-dep(1)/pks(1));
% %%
% zeta1=0:.01:1;
% PO_s_theory_1=100.*exp(-zeta1.*pi./(sqrt(1-(zeta1.^2))));
%
% figure
% plot(zeta1,PO_s_theory_1)
% xlabel('zeta')
% ylabel('Percent Overshoot')
% grid on

%% Rotate to Angle of Attack

[F,V,N] =stlread('SplitTip_CFD_3.25in_00degBinary.STL');
%[F,V,N] =stlread('TwistCap2degFillet0aoaBinary.STL');
aoa1 = 90; %in degrees angle of attack
```

```
aoa = -12; %in degrees angle of attack
dX=V(:,1);
dY=V(:,2)-min(V(:,2));
dZ=V(:,3);
ytake = dX;
ztake = dY;
xtake = dZ;
% be careful of return coordinates being in same zon
out1 = rodrigues_rot([xtake ytake ztake],[0 1 0],deg2rad(aoa1));
out = rodrigues_rot([out1(:,1) out1(:,2) out1(:,3)],[1 0 0],deg2rad(aoa));
dZ= out1(:,1);
dX= out(:,2);
dY = out(:,3);
%%
set(gcf,'Position',[700 400 1200 350]);
hold on
subplot(1,3,1)
plot(dZ,dX,'-*','Markersize',2)
xlabel('Z (meters)','Fontsize',14)
ylabel('X (meters)','Fontsize',14)
grid on
subplot(1,3,2)
plot(dZ,dY,'-*','Markersize',2)
xlabel('Z (meters)','Fontsize',14)
ylabel('Y (meters)','Fontsize',14)
grid on
subplot(1,3,3)
plot(dX,dY,'-*','Markersize',2)
xlabel('X (meters)','Fontsize',14)
ylabel('Y (meters)','Fontsize',14)
grid on
hold off
%% Write File
fid = fopen('Foil12deg.stl','w');
% plot(zn,yn)
% Write HEADER
fprintf(fid,'solid Simple_Foil\r\n');

hold on
for n = 1:length(F); %loops through top half

        P1(n,:) = [dX(F(n,1)) dY(F(n,1)) dZ(F(n,1))];
        P2(n,:) = [dX(F(n,2)) dY(F(n,2)) dZ(F(n,2))];
        P3(n,:) = [dX(F(n,3)) dY(F(n,3)) dZ(F(n,3))];

        %calculates normals to the two triangles
        V(n,:)=P2(n,:)-P1(n,:);
        W(n,:)=P3(n,:)-P1(n,:);
        N(n,:)=cross(V(n,:),W(n,:));

        fprintf(fid,'    facet normal %.7E %.7E %.7E\r\n',N(n,:));
        fprintf(fid,'        outer loop\r\n');
        fprintf(fid,'            vertex %.7E %.7E %.7E\r\n',P1(n,:));
        fprintf(fid,'            vertex %.7E %.7E %.7E\r\n',P2(n,:));
        fprintf(fid,'            vertex %.7E %.7E %.7E\r\n',P3(n,:));
        fprintf(fid,'        endloop\r\n');
```

```
        fprintf(fid,'    endfacet\r\n');
end

fprintf(fid,'endsolid')
fclose('all')
%% Experimental Data
EndCap=[0,-
0.0743940309371050,0.0303270565599566;3,0.0787544432067757,0.0405355998897566
;6,0.241533462743437,0.0545854114010836;9,0.366729659228409,0.098012222068909
1;12,0.508076341939926,0.137878856937000;15,0.619368581351845,0.1572259482331
46;18,0.703011739199905,0.206957319684205;21,0.634901323625603,0.348459667676
614];
General=[0,3,6,9,12,15,18,21;0.0223402871486852,0.170871967728479,0.328743872
558537,0.450165921129786,0.587251585514510,0.695188823856245,0.77631048617526
7,0.710253318144099;0.0303270565599566,0.0405355998897566,0.0545854114010836,
0.0980122220689091,0.137878856937000,0.157225948233146,0.206957319684205,0.34
8459667676614];
%General=[0,-
0.0506021441414626,0.0179537599935283;3,0.116017797477382,0.0241120083115157;
6,0.294732124723320,0.0447753111747490;9,0.465280749981846,0.0801202091750058
;12,0.625261450761526,0.139829948618632;15,0.762109188197743,0.15649191126172
2;18,0.874738968870083,0.199401415879689;21,0.809029695484579,0.3274403786987
25];
SplitTip=[0,-
0.0569820113359327,0.0238175932878067;3,0.120039653630706,0.0358385524000228;
6,0.292227331205562,0.0561666789666992;9,0.434013535373805,0.0763378706716329
;12,0.592523225365635,0.107234855772524;15,0.725175100832686,0.15639835166434
5;18,0.793757257497640,0.183466588354130;21,0.774096227073033,0.3041258230274
21];
SplitTipReversed=[0,-
0.0114833713924458,0.0425907308910981;3,0.159176969266030,0.0402227068301220;
6,0.311936141736373,0.0507673502440782;9,0.452497706175609,0.0678841799970550
;12,0.612682960204291,0.0904316294720582;15,0.725955071743894,0.1384052463695
69;18,0.813660618177823,0.185874869039129;21,0.771031085089715,0.289936872422
137];
%% OpenFoamData
EndCapO=[0,0.000357840990150000,0.039789509733000;3,0.160000000000000,0.0480
000000000000;6,0.277138646400000,0.061427083360000;9,0.344440005890000,0.086
1252267400000;12,0.440987378220000,0.127836124440000;15,0.503405541480000,0.1
65994949010000;18,0.535996123940000,0.228684382890000;21,0.473105560870000,0.
280757831870000];
GeneralO=[0,0.0275608397051437,0.045166129776812 4;3,0.219925968019401,0.05618
55727437665;6,0.349242566913294,0.071151719869912 2;9,0.438234576560000,0.0996
847443597445;12,0.585559569090000,0.138126712166627;15,0.649391397410000,0.17
2652449395329];
SplitTipO=[0,0.0380305270825149,0.046742151691940 6;3,0.206845960540594,0.0554
573458869505;6,0.331827372389703,0.073404809739099 0;9,0.445186765870000,0.106
082921109010;12,0.457683804968614,0.151073102535941];

EndClCd=(EndCap(:,2)./EndCap(:,3));
EndClCdO=(EndCapO(:,2)./EndCapO(:,3));
GeneralClCd=(General(2,:)./General(3,:));
GeneralClCdO=(GeneralO(:,2)./GeneralO(:,3));
SplitTipClCd=(SplitTip(:,2)./SplitTip(:,3));
SplitTipClCdReversed=(SplitTipReversed(:,2)./SplitTipReversed(:,3));
SplitTipClCdO=(SplitTipO(:,2)./SplitTipO(:,3));
```

```
figure
subplot(3,1,1)
plot1=plot(EndCap(:,1),EndCap(:,2),'-*k')
hold on
plot2=plot(EndCapO(:,1),EndCapO(:,2),'-or')
%set(gca,'FontSize',20)
title('End Cap')%,'FontSize',20)
ylabel('C_{Lift}')%,'FontSize',20)
axis([0 12 -.1 .7])
grid minor
%set(plot1(1),'Marker','*')%,'LineWidth',5,'LineStyle','-','LineWidth',2)
%set(plot2(1),'Marker','o')%,'LineWidth',5,'LineStyle','-','LineWidth',2)
subplot(3,1,2)
plot7=plot(EndCap(:,1),EndCap(:,3),'-*k')
hold on
plot8=plot(EndCapO(:,1),EndCapO(:,3),'-or')
grid minor
axis([0 12 0 0.2])
ylabel('C_{Drag}')%,'FontSize',20)
legend('Experimental','OpenFOAM','location','best')
%set(gca,'FontSize',20)
%set(plot7(1),'Marker','*','LineWidth',5,'LineStyle','-','LineWidth',2)
%set(plot8(1),'Marker','o','LineWidth',5,'LineStyle','-','LineWidth',2)
subplot(3,1,3)
plot13=plot(EndCap(:,1),EndClCd,'-*k')
hold on
plot14=plot(EndCapO(:,1),EndClCdO,'-or')
ylabel('C_{Lift}/C_{Drag}')%,'FontSize',20)
xlabel('Angle of Attack [deg]')
axis([0 12 -2 8])
grid minor
%set(gca,'FontSize',20)
%set(plot13(1),'Marker','*','LineWidth',5,'LineStyle','-','LineWidth',2)
%set(plot14(1),'Marker','o','LineWidth',5,'LineStyle','-','LineWidth',2)
figure
subplot(3,1,1)
plot3=plot(General(1,:),General(2,:),'-*k')
hold on
plot4=plot(GeneralO(:,1),GeneralO(:,2),'-or')
title('General Foil')%,'FontSize',30)
axis([0 12 -.1 .7])
grid minor
ylabel('C_{Lift}')
%set(gca,'FontSize',20)
%set(plot3(1),'Marker','*','LineWidth',5,'LineStyle','-','LineWidth',2)
%set(plot4(1),'Marker','o','LineWidth',5,'LineStyle','-','LineWidth',2)
subplot(3,1,2)
plot9=plot(General(1,:),General(3,:),'-*k')
hold on
plot10=plot(GeneralO(:,1),GeneralO(:,3),'-or')
axis([0 12 0 0.2])
grid minor
ylabel('C_{Drag}')
%set(gca,'FontSize',20)
legend('Experimental','OpenFOAM','location','best')
%set(plot9(1),'Marker','*','LineWidth',5,'LineStyle','-','LineWidth',2)
%set(plot10(1),'Marker','o','LineWidth',5,'LineStyle','-','LineWidth',2)
```

```
subplot(3,1,3)
plot15=plot(General(1,:),GeneralClCd,'-*k')
hold on
plot16=plot(GeneralO(:,1),GeneralClCdO,'-or')
axis([0 12 -2 8])
xlabel('Angle of Attack [deg]')%,'FontSize',30)
grid minor
ylabel('C_{Lift}/C_{Drag}')
%set(gca,'FontSize',20)
%set(plot15(1),'Marker','*','LineWidth',5,'LineStyle','-','LineWidth',2)
%set(plot16(1),'Marker','o','LineWidth',5,'LineStyle','-','LineWidth',2)
figure
subplot(3,1,1)
plot5=plot(SplitTipReversed(:,1),SplitTipReversed(:,2),'-*k')
hold on
plot6=plot(SplitTipO(:,1),SplitTipO(:,2),'-or')
axis([0 12 -.1 .7])
grid minor
ylabel('C_{Lift}')
%set(gca,'FontSize',20)
title('Split Tip')%,'FontSize',240)
%set(plot5(1),'Marker','*','LineWidth',5,'LineStyle','-','LineWidth',2)
%set(plot6(1),'Marker','o','LineWidth',5,'LineStyle','-','LineWidth',2)
subplot(3,1,2)
plot11=plot(SplitTip(:,1),SplitTip(:,3),'-*k')
hold on
plot12=plot(SplitTipO(:,1),SplitTipO(:,3),'-or')
axis([0 12 0 0.2])
grid minor
ylabel('C_{Drag}')
legend('Experimental','OpenFOAM','location','best')
%set(gca,'FontSize',20)
%set(plot11(1),'Marker','*','LineWidth',5,'LineStyle','-','LineWidth',2)
%set(plot12(1),'Marker','o','LineWidth',5,'LineStyle','-','LineWidth',2)
subplot(3,1,3)
plot17=plot(SplitTipReversed(:,1),SplitTipClCdReversed,'-*k')
hold on
plot18=plot(SplitTipO(:,1),SplitTipClCdO,'-or')
axis([0 12 -2 8])
grid minor
xlabel('Angle of Attack [deg]')
ylabel('C_{Lift}/C_{Drag}')
%set(gca,'FontSize',20)
%set(plot17(1),'Marker','*','LineWidth',5,'LineStyle','-','LineWidth',2)
%set(plot18(1),'Marker','o','LineWidth',5,'LineStyle','-','LineWidth',2)
% figure
% plot(EndCap(1,:),EndCap(2,:),'-*b',EndCap(1,:),EndCap(3,:),'-
*r',EndCapO(:,1),EndCapO(:,2),'--ob',EndCapO(:,1),EndCapO(:,3),'--or')
% legend('Experimental Lift','Experimental Drag','OpenFOAM Lift','OpenFOAM
Drag','location','best')
% xlabel('Angle Of Attack [deg]')
% ylabel('Coefficient of Lift/Drag')
% title('HiCaT Endcap 5m/s')
% axis([0 22 -.1 1])
%% coefficient of Drag
figure
[ax,h1,h2]=plotyy(General(1,:),General(2,:),General(1,:),General(3,:))
```

```
set(h1,'marker','*','color','red','linewidth',1)
set(h2,'marker','*','color','blue','linewidth',1)
hold on
[ax1,h11,h22]=plotyy(General0(:,1),General0(:,2),General0(:,1),General0(:,3))
set(h11,'marker','o','color','red','linestyle','--','linewidth',1)
set(h22,'marker','o','color','blue','linestyle','--','linewidth',1)

legend('Experimental Lift','Experimental Drag','OpenFOAM Lift','OpenFOAM
Drag','location','best')
xlabel('Angle Of Attack [deg]')
ylabel('Coefficient of Lift')
title('HiCaT General 5m/s')
axis([0 22 -.1 1 0 0.6])
```